Depolymerized Chitosan Nanoparticles for Protein Delivery: Preparation and Characterization

K. A. Janes, M. J. Alonso

Department of Pharmacy and Pharmaceutical Technology, School of Pharmacy, The University of Santiago de Compostela, 15706 Santiago de Compostela, Spain

Received 21 February 2001; accepted 30 August 2002

ABSTRACT: In this article we describe our preliminary work involving the use of depolymerized, low molecular weight chitosan nanoparticles as carriers for proteins and peptides. We hypothesized that the molecular weight of chitosan could favorably modulate the particle and protein release characteristics for the delivery of certain bioactive macromolecules. Our primary objectives were to develop nanoparticle formulations that were stable and reproducible across a range of chitosan molecular weights and then characterize the physicochemical and *in vitro* release properties as functions of the polymer size. Using depolymerized fragments generated by $NaNO_2$ degradation of different chitosan salts, we prepared nanoparticle formulations based on ionotropic gelation with sodium tripolyphosphate (TPP). Regardless of the formulation, the nanoparticle size decreased with decreasing molecular weight and the ζ-potential values remained unchanged. Similar comparisons were made with the encapsulation of insulin and tetanus toxoid as model proteins. The results indicated that the quantity of TPP in a given formulation has a greater effect on the protein encapsulation than the chitosan molecular weight. In fast release environments (i.e., buffered media), there was no significant molecular weight effect that could be discerned. These data lead to the conclusion that, under these experimental conditions, the chitosan molecular weight has a measurable effect on the particle properties, although this effect is modest relative to other formulation parameters (e.g., TPP content, type of protein loaded). Because these subtle differences could have dramatic effects physiologically, work is currently underway to elucidate the possible applications of depolymerized chitosans for peptide delivery *in vivo*. © 2003 Wiley Periodicals, Inc. J Appl Polym Sci 88: 2769–2776, 2003

Key words: chitosan; molecular weight; nanoparticles; peptide delivery; nasal delivery

INTRODUCTION

Chitosan (CS) is receiving increasing attention in the pharmaceutical field for a wide range of drug delivery applications.[1] α(1-4)2-Amino 2-deoxy β-D glucan (CS) is the deacetylated form of chitin, the second most abundant biopolymer in nature. In purified form, CS has many attractive features, including biocompatibility[2–4] and mucoadhesivity.[5–7] With an estimated intrinsic pK_a value of 6.5,[8] CS is also interesting from a technological point of view, because it is polycationic in acidic media and can interact with negatively charged species. This characteristic has been exploited for the formation of CS complexes and nanoparticulate structures with such polyanions as plasmid DNA[9–11] and proteoglycans.[12]

Recently, we have developed a CS nanoparticulate system via a mild ionotropic gelation procedure with sodium tripolyphosphate (TPP) as a counterion. This system has shown a high affinity for the association of negatively charged macromolecules, such as proteins[13,14] and oligonucleotides.[15] *In vivo*, these CS-TPP nanoparticles have shown promising results as nasal delivery vehicles for insulin[16] and antigens, such as tetanus toxoid,[17] where a prompt, facilitated administration of therapeutic proteins is desirable. Additionally, recent data have shown that these nanoparticles can maintain their performance following lyophilization.[18]

Several studies have suggested that the molecular weight of CS is a determining factor for its molecular properties. Schipper et al.[7] reported that the molecular weight affects the ability of soluble CS to increase membrane permeability in Caco-2 cell cultures. In CSs with low ($\leq$65%) degrees of deacetylation, higher molecular weight polymers ($\geq$100 kDa) induced greater membrane permeability, although all samples with high degrees of deacetylation ($\geq$85%) increased in permeability, regardless of the molecular weight. Conversely, Henriksen et al.[19] recommended low molecular weight (45 kDa) CS solutions for promoting ocular mucoadhesion.

Similar studies on the effect of molecular weight have been performed with different CS particulate systems. Shiraishi et al.[20] thoroughly investigated the effect of molecular weight on the performance of in-

Correspondence to: M. J. Alonso (ffmjalon@usc.es).

Contract grant sponsor: Spanish government; contract grant number: 1FD97-2363.

domethacin loaded CS-TPP beads. The group found that low molecular weight CS beads (25 kDa) produced the most significant increase in bioavailability following oral administration in dogs relative to other CS molecular weights. For CS microspheres synthesized by sodium sulfate precipitation, Berthold et al.[21] observed the highest prednisolone sodium phosphate loading with the lowest molecular weight that was tested (70 kDa).

Amidst the work involving CS solutions, macrostructures, and microstructures, only one group has investigated the effects of molecular weight on CS nanostructures, demonstrating its influence on the stability and transfection efficacy of CS–DNA complexes.[11] Moreover, as the overwhelming majority of commercially available CSs have average molecular weights that are much higher than 50–70 kDa, very few groups have tested the feasibility of low molecular weight CS (<50 kDa) for drug delivery applications, despite reports of increased biocompatibility and hemocompatibility.[22] Consequently, the aim of our work was to reliably generate low molecular weight CS fractions with average molecular weights ranging from 10 to 40 kDa and test their performance as CS-TPP nanoparticulate carriers compared to the original polymer. First, we thoroughly investigated the depolymerization process, generating a model that could predict decreases in the molecular weight for a given extent of depolymerization. Second, we explored the effects of the depolymerization process on the physicochemical properties of two distinct CS-TPP formulations. Third, we chose insulin and tetanus toxoid as model proteins to study the effect of molecular weight on drug loading and release.

EXPERIMENTAL

Preparation and characterization of CS fragments

Seacure® hydrolactate (CS-L210; number-average molecular weight, M_n, = 150–170 kDa; 82% deacetylated) and Protasan® hydrochloride (CS-CL110, $M_n > 50$ kDa, 87% deacetylated) were purchased from Pronova Biopolymer. The CS was dissolved to 0.2% (w/v) in 1% (v/v) acetic acid or Milli-Q water (Milli-Q plus, Millipore Ibérica), depending upon the particular nanoparticle formulation (see below), and paper filtered to remove particulates. CS fragments were generated by sodium nitrite degradation according to Peniston and Johnson.[23] Briefly, varying quantities of 0.1% (w/v) $NaNO_2$ (Probus) were added to the CS solution at room temperature under magnetic stirring, and the reaction was left overnight to assure completion of the degradation. For CS-L210 samples dissolved in acetic acid, the reduced viscosity of the resulting solution was measured at four dilutions (1–0.2 g/L) in a capillary viscometer (Afora) at 30°C. All measurements were made in triplicate. The intrinsic viscosity was determined by linear extrapolation to infinite dilution and used with the appropriate Mark–Houwink–Sakurada parameters[24] to calculate a viscosity-average molecular weight (M_V). All calculations of the polymer concentration and solution ionic strength were adjusted to take into account that a CS acid salt was used, rather than the free base form.

Generation of molecular model

A Monte Carlo simulation of the depolymerization process was created using Matlab 5.1 (MathWorks, Inc.). The model assumes a sample population of 10^5 CS macromolecules that are distributed by a normal distribution of molecular weights with the following mean (μ) and standard deviation (σ):

$$\mu = M_V, \quad \sigma = \frac{M_V}{3}$$

For the starting molecular weights that were simulated, the model generated on the order of 10^6–10^7 β-1,4-glycosidic linkages. To simulate the depolymerization process, a percentage of these glycosidic linkages was cleaved at random to compare with the same mole percentage of $NaNO_2$ added experimentally. The polymer distribution was updated and the molecular weight was calculated accordingly. The model assumes equal accessibility and reactivity of all $NaNO_2$ reactive linkages in all CS molecules, although trial simulations were also performed taking into account the β-1,4-glycosidic linkages adjacent to acetylated residues, which are not susceptible to $NaNO_2$ cleavage (see Discussion). Following the simulation, a new average molecular weight was calculated from the depolymerized distribution.

Preparation of CS-TPP nanoparticles

Following depolymerization, fragments were used without further purification for particle formation via ionotropic gelation with sodium TPP (Sigma Chemicals). Two different protocols were adopted for the formation of CS-TPP nanoparticles, one with low TPP content and another with high TPP content. In the first formulation, nanoparticles were synthesized according to the method described by Fernández-Urrusuno et al.[16] Briefly, 400 μL of 0.084% TPP was added to 1 mL of 0.2% CS in water under magnetic stirring for a final CS/TPP ratio of 6/1 by weight. In the second formulation, CS was diluted to 0.175% (w/v) in 1% acetic acid (solvent necessary to stabilize the high TPP formulation), deacidified to pH 4.7–4.8 with 10*N* NaOH, and filtered with a 0.45 μm syringe filter. To 500 μL of this solution was added 100 μL of 0.291%

TPP under magnetic stirring for a final CS/TPP ratio of 3/1 by weight.

For the association of proteins to the nanoparticles, bovine insulin (Sigma Chemicals) was dissolved at 5 mg/mL in 0.01*N* NaOH and tetanus toxoid (kindly donated by the World Health Organization) obtained in solution at 4.2 mg/mL. Each protein solution was incubated with a TPP solution whose concentration maintained the volume ratios of the blank nanoparticle formulations. The insulin theoretical loading in all cases was 30% (w/w) relative to the amount of CS and that of tetanus toxoid was 10% (w/w).

Physicochemical characterization of nanoparticles

Size and ζ-potential measurements were performed by photon correlation spectroscopy and laser Doppler anemometry, respectively, with a Zetasizer® 3000HS (Malvern Instruments). For size measurements, the samples were diluted in water and measured for a minimum of 180 s. Raw data was subsequently correlated to mean hydrodynamic size by cumulants analysis. For the ζ-potential measurements, samples were diluted in 0.1 m*M* KCl and measured in automatic mode. All measurements were performed in triplicate.

The particle morphology was examined by transmission electron microscopy (TEM; CM12 microscope, Philips, Eindhoven, The Netherlands). Samples were stained with 2% phosphotungstic acid for 10 min, immobilized on copper grids, and dried overnight for viewing.

Evaluation of protein loading capacity and yield

The encapsulation efficiency and nanoparticle yield of the insulin formulations were determined by centrifugation of the samples at 24,000 $\times$ *g* for 30 min. The pellets were dried at 80°C and weighed to calculate the yield. Supernatants were analyzed by the microBCA protein assay (Pierce) to determine the free protein concentration. For tetanus toxoid formulations, the supernatants of a concentrating centrifugation were used (9000 $\times$ *g*, 40 min), and the dry weights were not calculated. Calibration curves were made with corresponding solutions of blank nanoparticles, and all batches were measured in triplicate. The encapsulation efficiency was determined by difference as follows:

$$\text{encapsulation efficiency} = \frac{\text{total protein} - \text{free protein}}{\text{total protein}}$$

Evaluation of *in vitro* release

Insulin nanoparticles were concentrated by centrifugation at 10,000 $\times$ *g* for 40 min on a 5 μL glycerol bed.

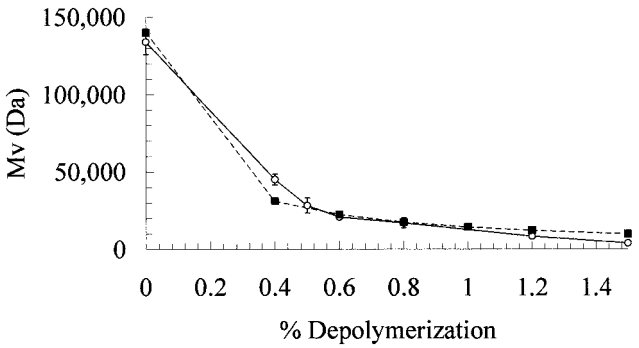

Figure 1 A comparison of the viscosimetry measurements (○) with the molecular model (■) for CS-L210 depolymerization.

The nanoparticles were resuspended and incubated in 1.5 mL of pH 4.0 acetate buffer at 37°C under light agitation. This release medium was chosen because it maintained the stability of both the particles and the released insulin the most effectively over the time period investigated. To make comparisons between depolymerized formulations, the quantity of nanoparticles was adjusted to a fixed quantity, which maintained sink conditions in all cases (15–25 μg/mL). At varying time points, the supernatants were isolated by centrifugation at 24,000 $\times$ *g* for 30 min and measured by the microBCA protein assay.

Statistical analysis

The confidence intervals (95%) for the intrinsic viscosity calculations were determined by support plane analysis[25] of the least squares fits for the different polymer solutions. All other results are displayed as the mean $\pm$ standard deviation. Statistical significance was assessed via a two-tailed Student's *t* test.

RESULTS

Viscosimetry and molecular model

Straight-line fits were obtained for all CS-L210 fragments ($R^2 > 0.9$). Using an estimated ionic strength of 5 m*M* (contributed by the acetic acid and acid salt), the Mark–Houwink–Sakurada parameters were calculated to be $k = 7.189 \times 10^{-4}$ L/g and $a = 0.6727$.[24] As the degrees of deacetylation for both CS-L210 and the CS used in Tsaih and Chen[24] were similar (82 and 83%, respectively), the effects of the degrees of deacetylation on Mark–Houwink–Sakurada parameters[26,27] were considered negligible. The M_V calculations of the undepolymerized CS-L210 gave an estimated molecular weight of 134 kDa.

To test the validity of the molecular simulation against these viscosimetric measurements, we used the hydrolactate CS salt with an assumed mean molecular weight of 140 kDa. Figure 1 shows the com-

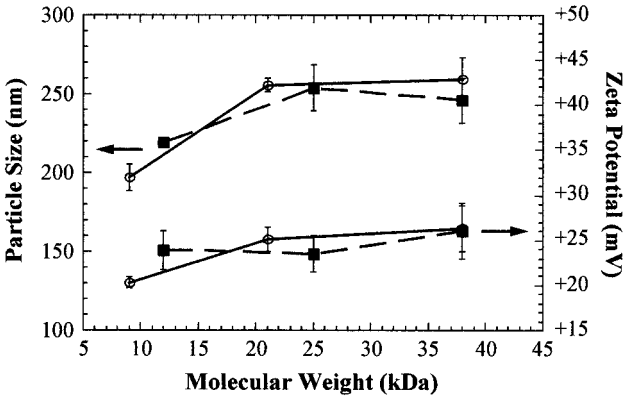

Figure 2 The particle size and ζ potential measurements of (○) CS-L210 and (■) CS-CL110 nanoparticles with the 3/1 CS/TPP formulation ($n = 3$).

parison between the model predictions and the actual viscosity measurements.

Nanoparticle characterization

We created three CS-L210 fragments with calculated molecular weights of 38, 21, and 9 kDa (0.4, 0.6, and 1.2 mol % depolymerization, respectively). Additionally, we used the molecular model to generate three CS-CL110 fractions with theoretical molecular weights of 38, 25, and 12 kDa, corresponding to respective fractional depolymerizations of 0.2, 0.4, and 1.1 mol %. We compared the physicochemical properties of nanoparticles (3/1 CS/TPP formulation) synthesized from different molecular weight fragments of CS-L210 and CS-CL110.

Figure 2 shows the influence of the polymer molecular weight on the size and ζ-potential values of nanoparticles made from the two polymers. Significant decreases in the particle size ($p < 0.05$) were noted only for the lowest molecular weight fragments of the two CS salts, although all fragments formed smaller particles than the corresponding, undepolymerized CS (data not shown). The ζ-potential values were largely independent of the molecular weights of both polymers, with the lowest molecular weight CS-L210 polymer showing a small, yet significant ($p < 0.01$) decrease relative to the other CS-L210 samples. The reaction yields of blank, low molecular weight nanoparticle formulations were similar with the same polymer, but CS-CL110 consistently gave higher yields (80–90%) than the corresponding CS-L210 formulation (60–70%).

With CS-CL110 fragments, we subsequently compared the effect of the molecular weight on the physicochemical properties of nanoparticles synthesized at two distinct CS/TPP ratios (6/1 and 3/1). Figure 3 shows the TEM image of particles from a typical formulation. The morphology of nanoparticles made from depolymerized CS-CL110 was nearly identical to that of the starting polymer (data not shown). Both suspensions contained dense, well-defined, spherical structures that were consistently observed, regardless of the CS/TPP ratio (data not shown). Figure 4 shows the size and ζ-potential values of the two formulations. Substantial increases were seen in both the particle size and ζ-potential ranges for the 6/1 CS/TPP formulation relative to the 3/1 CS/TPP one (200–250 to 280–360 nm and +20–28 to +40–48 mV, respectively). A gradual decrease in the particle size with the molecular weight was noted for both formulations, as in the previous study, but no significant changes were seen in the ζ potential.

Protein encapsulation

The insulin encapsulation efficiencies for the 3/1 and 6/1 CS/TPP formulations are shown in Table I. The 6/1 CS/TPP formulation showed encapsulation efficiencies between 75 and 85% and yields of 25–35%. The encapsulation efficiencies increased gradually with decreasing molecular weight and there were significant differences observed between the original polymer and the two lowest M_V fractions ($p < 0.01$), but no effect was observed in the case of the reaction yield. Conversely, the 3/1 CS/TPP formulation demonstrated encapsulation efficiencies of 10–35% and yields of 80–100%. For this particle formulation, there was no clear effect of molecular weight on either the encapsulation efficiency or yield, but all depolymerized samples showed slightly higher encapsulation efficiencies ($p < 0.1$) and lower yields than the original polymer.

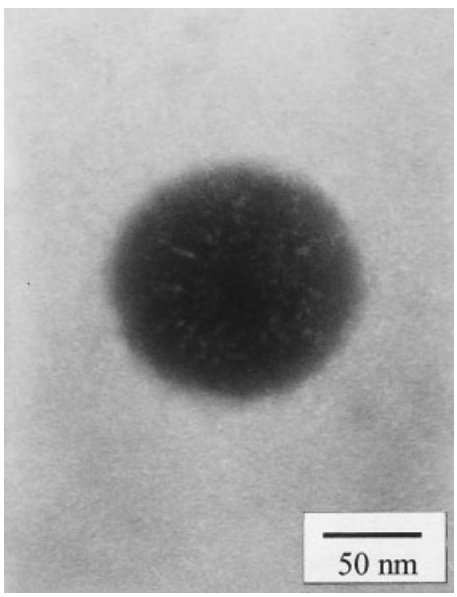

Figure 3 A transmission electron micrograph of CS-CL110 nanoparticles (6/1 CS/TPP formulation).

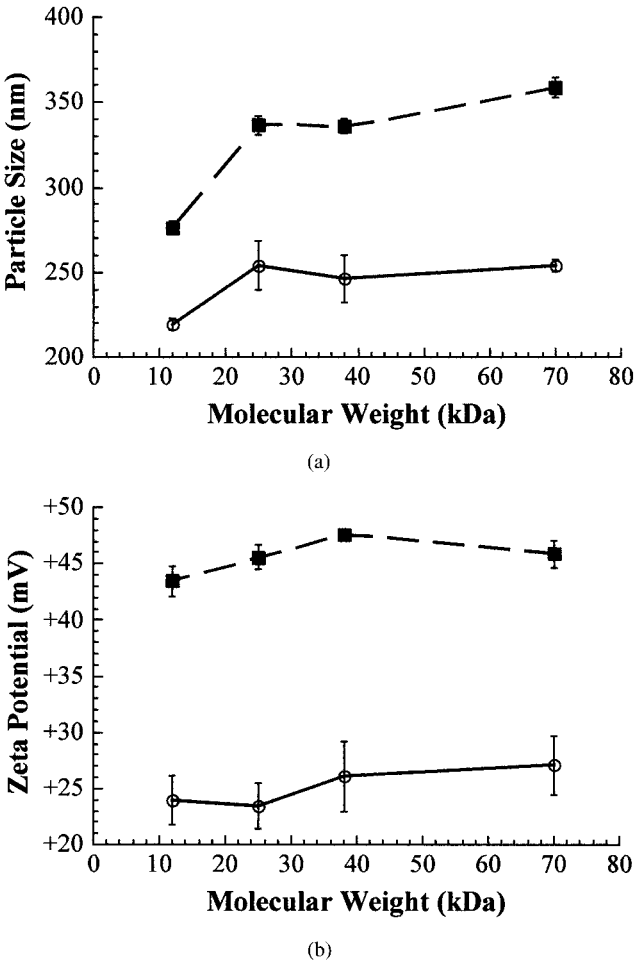

Figure 4 (A) Particle size measurements of (○) 3/1 and (■) 6/1 CS-CL110/TPP formulations ($n = 3$). (B) Particle ζ potential measurements of (○) 3/1 and (■) 6/1 CS-CL110/TPP formulations ($n = 3$).

Table II shows the encapsulation efficiencies of tetanus toxoid for the different nanoparticle formulations. The tetanus toxoid association was similar, irrespective of the M_V of CS for the 6/1 CS/TPP formulation, but slight, yet significant, increases were observed with depolymerized samples for the 3/1 CS/TPP formulation ($p < 0.05$). The encapsulation efficiencies for all formulations tested fell between approximately 45 and 55%.

TABLE II
Tetanus Toxoid Encapsulation Efficiencies for CS-CL110 High and Low TPP Formulations ($n = 3$)

CS M_V (kDa)	Formulation (%)	
	6/1 CS/TPP	3/1 CS/TPP
70	55.1 ± 3.4	45.1 ± 0.9
38	44.3 ± 5.5	51.3 ± 1.4
23	52.8 ± 1.9	55.4 ± 1.0

The theoretical loading is 10%.

In vitro release

The *in vitro* release profile for insulin loaded nanoparticles (6/1 CS/TPP) is depicted in Figure 5. For all molecular weights, 70–85% of the loaded insulin was released within the first 15 min of incubation in acetate buffer, and there was no significant effect of CS molecular weight. Time points were not continued beyond 30 min, because the insulin release had already appeared to plateau relative to the release observed after 15 min.

DISCUSSION

The aim of the depolymerization studies was to generate molecular weight fragments with M_V = 10–40 kDa from a starting CS salt of high molecular weight. A great advantage of the sodium nitrite method for CS degradation is that the number of glycosidic linkages broken is stoichiometric with the moles of $NaNO_2$ added, so the degree of depolymerization can be accurately controlled. *A priori*, however, it was difficult to predict the percentage of linkages that needed to be cleaved in order to generate these desired fractions. Because $NaNO_2$ is not capable of cleaving linkages adjacent to *N*-acetylglucosamine residues, we were additionally concerned if the remaining acetylated residues would affect these predictions. In an effort to resolve these questions, we created a molecular model

TABLE I
Insulin Encapsulation Efficiencies ($n = 3$) and Blank Nanoparticle Yields ($n = 1$) for 6/1 and 3/1 CS-CL110/TPP Formulations

CS M_V (kDa)	6/1 CS/TPP Formulation		3/1 CS/TPP Formulation	
	Encapsulation efficiency (%)	Yield (%)	Encapsulation efficiency (%)	Yield (%)
70	77.1 ± 0.5	102	11.1 ± 5.8	36
38	78.7 ± 1.5	84	36.3 ± 6.1	26
23	81.3 ± 0.7	90	23.6 ± 8.6	28
12	83.7 ± 1.2	84	20.7 ± 2.7	35

The theoretical loading is 30%.

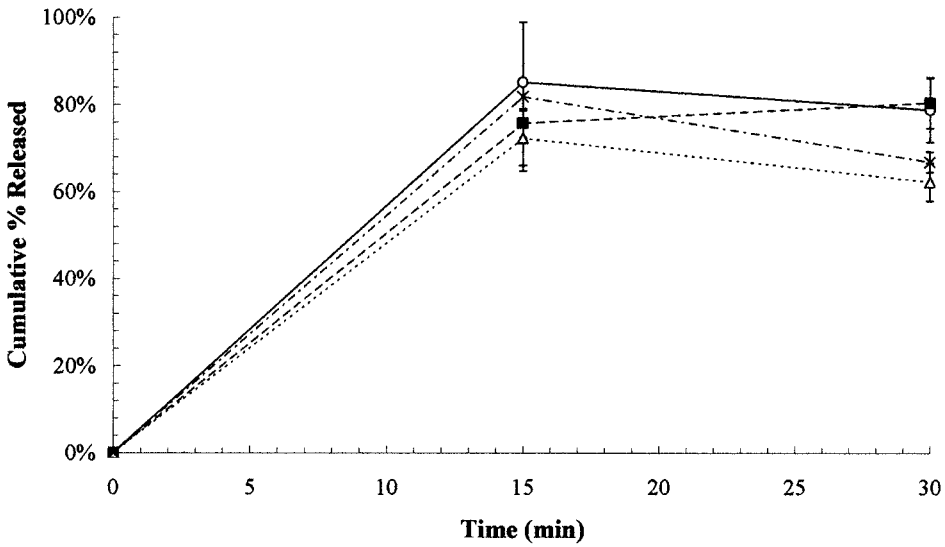

Figure 5 Insulin release profiles for the CS-CL110 high TPP formulation at (○) 70, (■) 38, (△) 25, and (×) 12 kDa (n = 3).

that would attempt to predict the M_V for a particular extent of depolymerization.

Beforehand, we tested the accuracy of the viscosimetry setup. The molecular weight calculated by the viscosity was slightly lower than that provided by the manufacturer (150–170 kDa). We compared the M_V versus the percentage of depolymerization curve predicted by the simulation to that generated by viscosity measurements of actual depolymerized samples. Figure 1 shows that the model predicts the M_V values calculated by viscosimetry quite well, particularly in the lower molecular weight range of interest (10–30 kDa). Deviations below this limit are likely due to a breakdown in the applicability of the Mark–Houwink–Sakurada parameters, which have a range of about 2 orders of magnitude.[28] Because the parameters calculated in Tsaih and Chen[24] employed CSs up to 914 kDa, estimations below 10 kDa with the same a and k values are likely problematic.

Changing the degree of acetylation from low to moderate values (0–20%) in the simulation did not significantly change the predicted average molecular weight, because of the small extents of depolymerization explored. Since the moles of available linkages were always in far excess of the moles of $NaNO_2$ in the system, a minimal effect of acetylated residues should be observed on the molecular weight average. Analogously, because only a small fraction of linkages were ultimately cleaved in this study, the changes in the polymer properties due net increases in acetylation of the depolymerized samples per unit weight relative to the original polymer can be considered negligible, in accordance with previous reports.[11]

Although viscosimetric measurements of all CS-L210 fragments were possible, it was not the case with measurements of the hydrochloride salt under the same conditions. We observed bi- and triphasic reduced viscosity versus concentration curves similar to that reported previously for other cationic polymers.[29] The reason for the differences in the rheological behavior of CS-L210 and CS-CL110 is not clear, but they could be due to differences in the initial molecular weight (150–170 vs. 60–90 kDa), degrees of acetylation (82 vs. 87%), purity (low vs. high), or salt type (hydrolactate vs. hydrochloride). The same irregular behavior was encountered with CS-CL110 using a higher ionic strength medium recommended by the manufacturer (0.02M NaAc/HAc buffer + 0.1M NaCl).[30]

Predictions of the simulation would be considered to be more robust than the viscosimetry data following a change in a polymer of this nature, because the actual depolymerization events are independent of the salt type and ionic strength, as is the case with the simulation, whereas the intrinsic viscosity calculations of the resulting molecular weight are highly sensitive to these variables. Notwithstanding, in the instances where straight-line extrapolations of the intrinsic viscosity were achieved with CS-CL110 (moderate depolymerizations), the model provided a reasonable prediction of the calculated M_V (data not shown). As a result, the molecular simulation with an assumed M_V of 70 kDa was used exclusively to approximate the molecular weights of the depolymerized CS-CL110 samples.

The size and ζ-potential values of nanoparticles made from CS-L210 and CS-CL110 fragments were compared. As can be seen in Figure 2, the size and ζ-potential values for the formulations were largely overlapping between the two polymers for corresponding molecular weights. The ζ-potential values were unchanged, and the drop in particle size with the molecular weight occurred at precisely the same mo-

lecular weight region and with the same magnitude. Both of these observations were expected, because it is logical that the size would decrease with the M_V, which is due to the decreased apparent viscosity of the CS solution and the increased ability of lower molecular weight CS to form smaller nanoparticulate structures. The fact that this decrease with the M_V was reflected in both CS-L210 (measured M_V) and CS-CL110 (predicted M_V) nanoparticles reinforces the correspondence of modeled and viscometric molecular weight calculations. Conversely, the ζ potential should remain constant, as the relative quantity of positively charged CS to negatively charged TPP was maintained constant.

From this point, we chose to work exclusively with the CS-CL110 fragments, because of the higher purity of the starting polymer and the observed increase in yield with respect to CS-L210 nanoparticles. We compared the 3/1 CS/TPP formulation with a previously published[16] formulation for insulin delivery containing half the amount of TPP by mass. The dramatic increase in particle size and ζ potential, as well as the decrease in the yield seen with this latter formulation, are likely attributable to this difference. With less TPP, the available anions are less able to neutralize the positive charge of CS and condense the polymer into tight particulates, thus creating a lower amount of larger, more positively charged structures. Despite this change, the trends with the molecular weight were identical to those observed earlier (i.e., a gradual decrease in particle size with molecular weight and no change in the ζ potential).

We compared the loading ability of the two formulations using insulin as a model protein. The results in Table I clearly demonstrate the importance of a high CS concentration relative to TPP in the formulation to achieve high encapsulation efficiencies of insulin for the chosen loading level. The low yield 6/1 CS/TPP formulations encapsulated dramatically higher quantities of insulin than the corresponding 3/1 CS/TPP formulation. Additionally, the encapsulation efficiencies for the 3/1 CS/TPP formulation appeared to proceed inversely with the yield for the molecular weights we tested. This phenomenon can be explained by the mechanism of protein encapsulation for the CS-TPP system, which is believed to occur via electrostatic interactions between the negative residues on the protein (which is maintained at a pH above its pI) and the amino groups of CS. Assuming 100% protonation of primary amines of CS-CL110 (a valid assumption given the acidic pH of the nanoparticle solution), complete charge neutralization of CS with TPP in a blank nanoparticle formulation can be expected to occur at a CS/TPP ratio of 2.34/1 by weight. The 3/1 CS/TPP formulation therefore contains only a slight excess of CS. As a blank nanoparticle suspension, the TPP in the formulation gelates nearly all of the CS, resulting in high yield particles. This close charge equivalence, however, leaves very few free positive amino groups that can entrap protein. Because TPP is a much smaller molecule with a higher charge density, it completely dominates competition with the protein for CS, dramatically reducing the encapsulation efficiency.

Such a drastic effect of the blank nanoparticle yield on the encapsulation efficiency should not be expected for all proteins. As seen in Table II, the quantity of TPP had very little effect on the encapsulation of tetanus toxoid. The cause for this is likely the difference in protein and theoretical loading levels. Tetanus toxoid is a much larger molecule than insulin (150 vs. 6 kDa), and 3 times less of the protein by weight was incorporated in the tetanus toxoid formulation (10 vs. 30% theoretical loading). Consequently, the amino groups of CS were not fully saturated, as in the case of insulin, because there were far fewer tetanus toxoid molecules to entrap. This indicates that the 3/1 CS/TPP formulation might remain applicable for the encapsulation of high molecular weight macromolecules at low loading levels.

The effects of the M_V on *in vitro* release were investigated using insulin as a model protein. We chose the 6/1 CS/TPP formulation to perform these studies, because it was able to encapsulate insulin more effectively at the desired loading levels. For insulin release in a buffered media, we noted a rapid and near complete release with all molecular weights within 15 min. Our hypothesis for this fast release is that anions in the medium compete with insulin for electrostatic interactions with CS. This competition screens the attractive forces retaining the protein within the particles, leading to a near immediate release.

However, true characterization of *in vivo* protein release by *in vitro* studies is difficult. Moreover, it is further complicated by the administration route of interest, because nasal protein release would occur on a mucosal surface rather than in the bulk. For this reason, we focused on a formulation whose *in vitro* characteristics were previously demonstrated to be sufficient to generate the desired behavior *in vivo*.[16] With this preestablished system, we could then explore any effects of the molecular weight on *in vitro* release in a systematic fashion. Because the highest CS molecular weight that we tested demonstrated an extremely rapid release profile, the potential influences of M_V that might be expected *a priori* (e.g., faster, more complete release) could not be discerned. However, it is important to stress that this does not preclude the possibility of the molecular weight influencing the behavior of these particles *in vivo*, where the lower molecular weight formulations might behave differently in the more complex environment. Indeed, preliminary work *in vivo* with low molecular weight CS nanoparticle delivery of tetanus toxoid has shown

measurable increases in immune response with decreasing molecular weight.[31]

CONCLUSION

We have demonstrated the ability to reliably generate low molecular weight CS from a starting CS salt of high molecular weight. CS depolymerization can be facilely controlled and modeled by simple molecular simulations in order to create fractions with a desired M_V. Depolymerized CS retains its ability to form nanoparticles via ionotropic gelation with TPP, and we observed that particular formulations demonstrate distinctive characteristics with respect to particle size and drug loading under certain conditions relative to the same formulation with the starting polymer. Furthermore, the majority of these trends were consistent with changes in the molecular weight. Consequently, these studies may indicate the possibility of using depolymerized CS to modulate *in vivo* nanoparticle behavior for certain applications. A modulation of this sort could not be discerned *in vitro*, but *in vivo* work is necessary to more fully test this hypothesis.

This work was supported by a grant from the Spanish government. The first author (K. A. J.) would like to thank the U.S.I.A. Fulbright Association.

References

1. Dodane, V.; Vilivalam, V. Pharmaceutical Science and Technology Today 1998, 1, 246.
2. Knapczyk, J.; Krówczynski, L.; Krzck, J.; Brzeski, M.; Nirnberg, E.; Schenk, D.; Struszcyk, H. In Chitin and Chitosan: Sources, Chemistry, Biochemistry, Physical Properties and Applications; Skak-Braek, G., Anthonsen, T., Sandford, P., Eds.; Elsevier: London, 1989; p 657.
3. Hirano, S.; Seino, H.; Akiyama, I.; Nonaka, I. In Progress in Biomedical Polymers; Gebelein, C. G., Dunn, R. L., Eds.; Plenum: New York, 1990; p 283.
4. Weiner, M. L. In Advances in Chitin and Chitosan; Brine, C. J., Sandford, P. A., Zikakis, J. P., Eds.; Elsevier: London, 1993; p 663.
5. Artursson, P.; Lindmark, T.; Davis, S. S.; Illum, L. Pharm Res 1994, 11, 1358.
6. Borchard, G.; Lueben, H. L.; De Boer, G. A.; Coos Verhoef, J.; Lehr, C. M.; Junginger, H. E. J Controlled Release 1996, 39, 131.
7. Schipper, N. G. M.; Vårum, K. M.; Artursson, P. Pharm Res 1996, 13, 1686.
8. Anthonsen, M. W.; Smidsrød, O. Carbohydr Polym 1995, 26, 303.
9. Leong, K. W.; Mao, H.-Q.; Truong-Le, V. L.; Roy, K.; Walsh, S. M.; August, J. T. J Controlled Release 1998, 53, 183.
10. Erbacher, P.; Zou, S.; Bettinger, T.; Steffan, A. M.; Remy, J. S. Pharm Res 1998, 15, 1332.
11. MacLaughlin, F. C.; Mumper, R. J.; Wang, J.; Tagliaferri, J. M.; Gill, I.; Hinchcliffe, M.; Rolland, A. P. J Controlled Release 1998, 56, 259.
12. Tian, X. X.; Groves, M. J. J Pharm Pharmacol 1999, 51, 151.
13. Calvo, P.; Remuñán-López, C.; Vila-Jato, J. L.; Alonso, M. J. J Appl Polym Sci 1997, 63, 125.
14. Calvo, P.; Remuñán-López, C.; Vila-Jato, J. L.; Alonso, M. J. Pharm Res 1997, 14, 1431.
15. Calvo, P.; Boughaba, A. S.; Appel, M.; Fattal, E.; Alonso, M. J.; Couvreur, P. Proc World Mtg APGI/APV 1998, 2, 1111.
16. Fernández-Urrusuno, R.; Calvo, P.; Remuñán-López, C.; Vila-Jato, J. L.; Alonso, M. J. Pharm Res 1999, 16, 1576.
17. Vila, A.; Sánchez, A.; Tobío, M.; Calvo, P.; Alonso, M. J. J Controlled Release 2002, 78, 15.
18. Fernández-Urrusuno, R.; Romani, D.; Calvo, P.; Vila-Jato, J. L.; Alonso, M. J. STP Pharm Sci 1999, 5, 429.
19. Henriksen, I.; Green, K. L.; Smart, J. D.; Smistad, G.; Karlsen, J. Int J Pharm 1996, 145, 231.
20. Shiraishi, S.; Imai, T.; Otagiri, M. J Controlled Release 1993, 25, 217.
21. Berthold, A.; Cremer, K.; Kreuter, J. J Controlled Release 1996, 39, 17.
22. Richardson, S. C. W.; Kolbe, H. V. J.; Duncan, R. Int J Pharm 1999, 178, 231.
23. Peniston, Q. P.; Johnson, E. L. U.S. Pat. 3,922,260, 1975.
24. Tsaih, M. L.; Chen, R. H. Int J Biol Macromol 1997, 20, 233.
25. Straume, M.; Frasier-Cadoret, S. G.; Johnson, M. L. In Topics in Fluorescence Spectroscopy, Principles; Lakowitz, J. R., Ed.; Plenum: New York, 1991; Vol. 2, p 177.
26. Rinaudo, M.; Milas, M.; Dung, P. L. Int J Biol Macromol 1993, 15, 281.
27. Wang, W.; Bo, S.; Li, S.; Qin, W. Int J Biol Macromol 1991, 13, 281.
28. Harding, S. E.; Vårum, K. M.; Stokke, B. T.; Smidsrød, O. In Advances in Carbohydrate Analysis; White, C. A., Ed.; JAI Press: London, 1991; p 63.
29. Ghimici, L.; Popescu, F. Eur Polym J 1998, 34, 13.
30. Anthonsen, M. W.; Varum, K. M.; Smidsrød, O. Carbohydr Polym 1993, 22, 193.
31. Vila, A.; Sánchez, A.; Janes, K. A.; Vila-Jato, J. L.; Alonso, M. J. Proc Int Symp Controlled Release Bioact Mater, 2001.